IEEE Access
Multidisciplinary | Rapid Review | Open Access Journal

SPECIAL SECTION ON DEEP LEARNING ALGORITHMS FOR INTERNET OF MEDICAL THINGS

Received March 23, 2020, accepted April 6, 2020, date of publication April 10, 2020, date of current version April 28, 2020.

Digital Object Identifier 10.1109/ACCESS.2020.2987058

Health Monitoring of Human Multiple Physiological Parameters Based on Wireless Remote Medical System

KAI ZHANG AND WENJIE LING
Sports Institute, Xinxiang Medical University, Xinxiang 453003, China

Corresponding author: Kai Zhang (zhangkai@xxmu.edu.cn)

This work was supported by a Key Project funded by Scientific Research of Institutions of Higher Learning in Henan Province under Grant 20A890009.

ABSTRACT Telemedicine, as a new technical means and medical model, can truly realize the sharing and monitoring of telemedicine information, and ultimately ensure that everyone has equal access to medical and health resources. Based on the research on the status of telemedicine application and wireless communication technology, this paper proposes a multi-physical parameter wireless telemedicine health monitoring system solution, and analyzes the overall structure and functional requirements of the system. Human physiological parameters of the wireless remote medical system for health monitoring include body temperature, respiration, blood oxygen saturation, pulse, blood pressure, and electrocardiogram. In this paper, fabric electrodes are used to extract human bioimpedance signals, discrete Fourier transform algorithm is used to detect human respiratory signals, and respiratory rate is detected based on dynamic differential threshold peak detection technology. The reflection type photoelectric sensor is used to realize the reflection of the human pulse signal, and the continuous measurement of the cuff-free blood pressure based on the pulse wave conduction time is combined with the ECG (Electrocardiogram) data. A self-learning threshold algorithm based on near-infrared photo plethysmo graphy signal trough detection is designed on the reflective blood oxygen saturation calculation algorithm. The difference threshold method is used to extract the QRS band feature points. We tested the overall operation of the system. The results show that the collected human physiological signal data is accurate. After a series of tests, the validity and reliability of the collected physiological signals have been proven.

INDEX TERMS Telemedicine, health monitoring, physiological signals, signal processing.

I. INTRODUCTION

Traditional medical technology often requires patients to come to the hospital for treatment in front of a doctor, which often requires the patient to have enough time, but it is very unsatisfactory for some irregular diseases, sudden diseases, and patients who need periodic care. In order to reduce the consequences of sudden illness, researchers around the world are stepping up research and development of effective telemedicine technologies [1]–[3]. Of course, as a technology of great significance, telemedicine can remotely monitor the patient's physiological condition in real time through a monitoring center, which can effectively control the spread of sudden infectious diseases to a large extent [4], [5].

Because the United States and Europe have incomparable satellite advantages, the first experimental platform used is satellite communication technology, and the area that benefits the most is Alaska, the farthest from the continental United States [6], [7]. The area is vast and sparsely populated, and medical resources are relatively scarce. Through the technical means of remote medical monitoring, the state's medical and health standards have been greatly improved [8]. In Europe, most countries use mobile communication technology as a platform for telemedicine [9], [10]. The reason is that on the one hand, Europe already has a very developed mobile communication network, and the technology is leading the world. On the other hand, it is because of the geographical

The associate editor coordinating the review of this manuscript and approving it for publication was Wei Wei.

environment of Europe that it can adopt mobile communication to achieve telemedicine [11]. At present, the telemedicine monitoring system adopted by the intensive patient monitoring center of the hospital affiliated with the University of Michigan in the United States also monitors patients, and Florida State Hospital has demonstrated the use of a wireless telemedicine monitoring system to provide monitoring for 3,000 beds [12]–[14]. Countries and regions such as South Africa, Japan, and Australia have also carried out various forms of telemedicine activities suitable for their own development [15]–[17]. The medical monitoring system researched in Greece is installed in an ambulance and communicates and connects with the hospital's remote monitoring center through the global mobile communication system network [18], [19]. This system can monitor the patient's physiological parameters at any time in order to obtain timely and effective guidance from experts [20]. In emergency situations, you can fight for rescue time. This system has been put into clinical use in Italy, Sweden, Cyprus, Greece and other countries, and the clinical effect is very good [21]–[23]. With the qualitative changes in communication quality and communication speed of wireless communication technology, various advanced communication technologies are being continuously adopted in the field of telemedicine [24], [25]. The gradual popularization of Wi-Fi networks has made Wi-Fi networks and the Internet a rapidly developing area [26]–[28]. Multi-network fusion technology will be more and more favored by research experts [29], [30]. Relevant scholars have studied the family intimate nurse system [31]–[33]. The system is mainly composed of a home monitor and a hospital console. The monitor has a built-in intelligent control system that can remotely record and record real-time ECG (Electrocardiogram) and ambulatory blood pressure values, and realize real-time analysis of cases. Once an abnormal heart rate appears, the user's ECG is transmitted to the hospital console via the telephone network for consultation and diagnosis by experts [34], [35]. The hospital console can simultaneously receive and display the ECG and blood pressure data of multiple home users, and immediately return diagnostic opinions and treatment plans to the home users [36]. In addition, related scholars have also conducted research on virtual medical data acquisition instruments based on the Internet [37], [38].

With the development of society, people have gradually increased their living requirements, and they have paid more and more attention to medical services. Due to the development of network technology and information technology, remote medical monitoring systems have also been greatly developed. It has played a role in making up for the lack of many traditional medical services. Based on medical electronic technology and sensor technology, this paper designs a multi-physical parameter wireless remote medical health monitoring system in the field of wireless sensor network applications. Specifically, the technical contributions of this paper can be summarized as follows:

First: After the respiratory signal is denoised, the respiratory rate is calculated from the peak value of the dynamic differential threshold. Based on pulse data and ECG data, the measurement of cuff-free blood pressure based on pulse wave transit time was studied. In view of the poor stability of the reflected pulse wave signal, a valley detection algorithm based on infrared light PPG (Photo Plethysmo Graphy) was designed to calculate the blood oxygen saturation value and pulse rate value. A QRS wave detection algorithm for ECG signals based on the differential threshold method was designed, and combined with the false detection and missed detection mechanism, a higher QRS wave detection rate was obtained.

Second: The entire system was tested and verified. The accuracy of physiological signals such as respiratory signals, ECG signals, pulse wave signals, and body temperature was verified, and the accuracy of the calculation algorithms for heart rate, breathing rate, heart rate, blood oxygen saturation, and blood pressure was verified.

The rest of this paper is organized as follows. Section 2 conducts research on telemedicine multi-physiological health monitoring system. Section 3 studies the physiological parameter signal processing and related algorithms. Section 4 tests the wireless telemedicine system and analyzes the results. Section 5 summarizes the full text and points out future research directions.

II. RESEARCH ON TELEMEDICINE MULTIPLE PHYSIOLOGICAL PARAMETER HEALTH MONITORING SYSTEM

A. STRUCTURE OF WIRELESS REMOTE MULTIPLE PHYSIOLOGICAL PARAMETER TRANSMISSION SYSTEM

The wireless remote physiological parameter transmission system belongs to the category of a remote monitoring system, and monitors physiological parameters reflecting human functions as needed [39]. If there is an abnormality, the body is reminded by an alarm on the one hand, and sent to the corresponding monitoring center through the global mobile communication system network. The monitoring center records relevant data, and if necessary, feeds back diagnostic opinions through the GSM network. The remote monitoring system is part of the medical network, as shown in Figure 1.

As shown in Figure 1, the integration of hospital information and global information forms an organic whole. The figure shows that the monitoring center can be located in the emergency center and the hospital. When the remote monitoring equipment detects the physiological parameters that need to be transmitted to the monitoring center, the communication system serves as a medium to complete the task of transmitting the physiological parameters to the relevant monitoring center. Through Bluetooth low energy technology, multiple physiological parameter detection nodes are connected to the intelligent terminal to form a master-slave star network structure. The physiological parameter data is

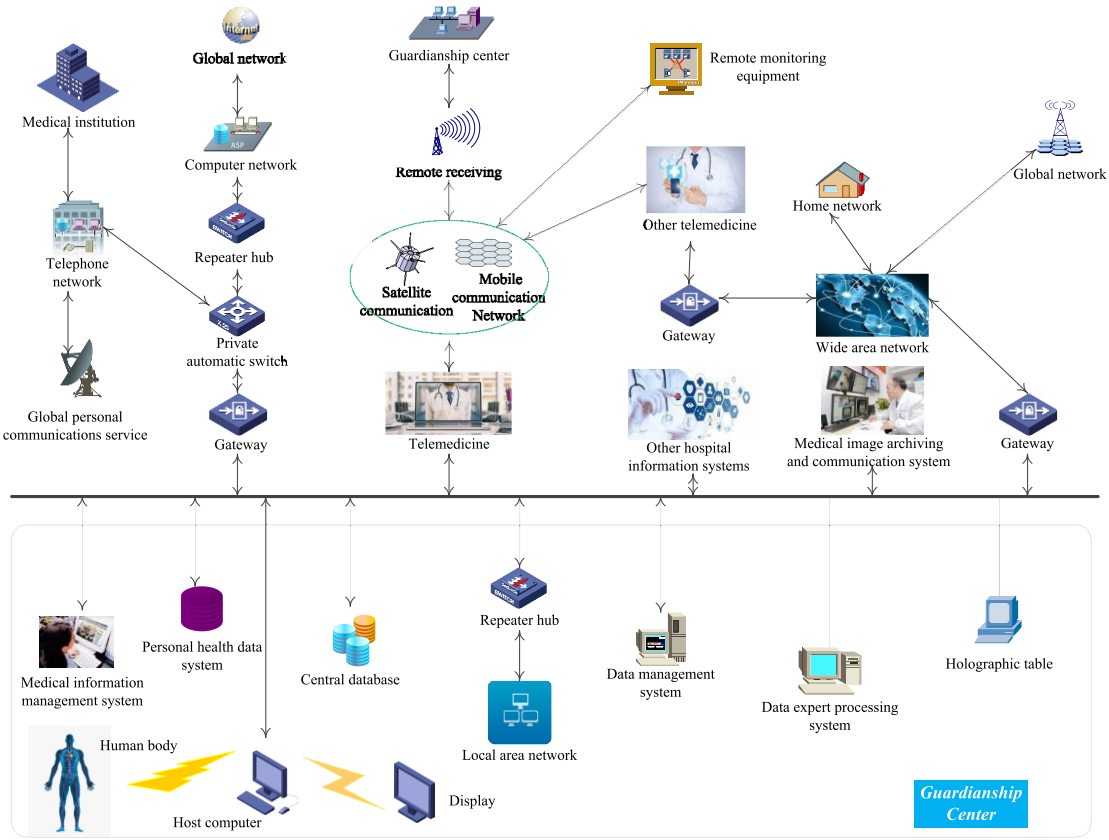

FIGURE 1. Schematic diagram of wireless telemedicine network.

transmitted to the remote terminal in real time, and then the data is processed, displayed and stored.

The wireless remote physiological parameter transmission system in this paper will use mobile communication technology. The monitoring object is not limited to patients, but ordinary healthy people can also pay attention to some physiological parameters. The monitoring area can be in an emergency medical situation, or it can be work at home or outside. Monitoring parameters can be either important physiological parameters of the patient or daily living conditions. Its fields of application range from the study of the physiological state of the human body under extreme conditions and first aid to family health care for millions of households.

In the wireless remote physiological parameter transmission system in this paper, the physiological parameters reflecting the function of the human body mainly include ECG, blood pressure, blood oxygen saturation, body temperature, breathing, etc. They have extremely important reference values in human life monitoring [40], [41]. Finding some early physiological parameter changes, and regulating and processing can reduce or even avoid accidents. Remote monitoring equipment measures these physiological parameters through OEM (Original Equipment Manufacturer) modules [42]. There are many companies that produce such specialized modules, which specialize in the exploration and research of a certain field, and the quality and performance of the products they produce are superior. The use of OEM modules can make full use of these existing resources and apply the latest scientific and technological achievements in a timely manner [43]. At the same time, it simplifies the structure of the product, significantly shortens the development cycle, and is conducive to improving the stability, reliability and maintainability of the instrument [44], [45].

The embedded microprocessor used in the remote monitoring equipment is S3C44B0X produced by Samsung Korea. First, adding a power circuit, a clock circuit, and a storage circuit to a S3C44B0X microprocessor constitutes an embedded core control module. Then, they fully expand the peripheral equipment and communication interface of S3C44B0X embedded microprocessor, spare RS-232-C interface, RS-485 serial interface, so that modules with different interface standards can exchange data with this system. Finally, based on the built hardware environment, embedded software based on the real-time operating system μC / OS-II is written to process and control the monitored physiological signals. Because the communication system chooses the global mobile communication system network, there is an important part in the remote monitoring equipment, which is the global mobile communication system module. In this part, Siemens TC35i is selected. The peripheral circuit is designed with

TC35i as the core, and it is made into a global mobile communication system modem, which exchanges data with the ARM (Advanced RISC Machine) terminal, so that remote monitoring equipment can be realized through the global mobile communication system network. The monitoring center uses another global mobile communication system modem based on TC35i to receive signals, and interacts with the PC through the RS-232-C series communication interface, thereby transmitting the remote physiological parameters to the PC at the monitoring center. The management system of the monitoring center can monitor multiple signal sources simultaneously. Once the connection is established, the visual program analyzes the received data. At the same time, the physiological condition of the body is diagnosed, and the diagnosis opinion is fed back to the remote user through the global mobile communication system network as needed. The system block diagram of the wireless remote physiological parameter transmission system is shown in Figure 2.

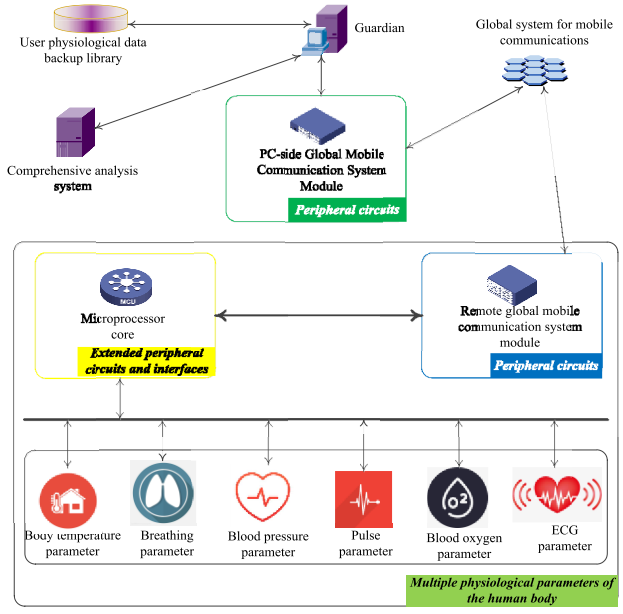

FIGURE 2. Block diagram of wireless remote physiological parameter transmission system.

B. MEASUREMENT OF MULTIPLE PHYSIOLOGICAL PARAMETERS OF THE HUMAN BODY

1) MEASUREMENT OF BODY TEMPERATURE

Based on the comparison of cost, sensitivity, and measurement accuracy, this system uses the YSI-400 thermistor temperature probe from Shenzhen Midland Electronic Technology Co., Ltd., which is mainly used to measure the body surface temperature with an accuracy of ± 0.1 °C. Thermistors are semiconductors based on ceramic materials and are divided into negative temperature coefficient thermistors and positive temperature coefficient thermistors. YSI-400 body temperature probe is a negative temperature coefficient thermistor and has a large negative temperature coefficient.

The standard resistance value of YSI-400 body temperature sensor is 2.25kΩ. Using the principle of resistance voltage division, a temperature sensor is connected in series with another precision resistor (2kΩ, 1%) R_1, one end is connected to a + 5V power supply, and the other end is grounded. The output interface of the temperature sensor uses a 6.36mm mono microphone plug, so a socket (female) with a matching interface structure is required. The sensor plug is a two-core, and the voltage signal at the output is sent to the P0.0 port of the CC2430. The AD port P0.0 of CC2430 collects the voltage signal TV across the YSI-400 body temperature sensor. Because the body temperature sensor and precision resistor R1 are connected in series, according to the principle that the current of the entire circuit is equal to the current on the YSI-400 body temperature sensor, there are:

$$\frac{V_{CC}}{R_T + R_1} = \frac{V_T}{R_T} \tag{1}$$

Among them, V_{CC} represents the power supply voltage + 5V, V_T represents the voltage across the YSI-400 body temperature sensor, and R_T represents the thermistor resistance of the body temperature sensor. It can be concluded that:

$$R_T = \frac{R_1 \cdot V_T}{V_{CC} - V_T} \tag{2}$$

Here, R_T is the thermistor resistance value of the YSI-400 body temperature sensor. The temperature-resistance table of the thermistor provided by the manufacturer can be obtained by checking the table.

2) MEASUREMENT OF BREATHING

The breathing measurement in this design is done in the ECG module. Breath measurement methods in the monitor include pressure-sensitive element method, heat-sensitive element method, and chest impedance method. The breathing measurement method involved in this design is the chest impedance method.

The thoracic movement of the human body during breathing will cause the impedance value between the two breathing electrodes to change. During measurement, a sine wave constant current source with a carrier frequency of 10K-100KHZ is injected into the human body through the two heart electrodes of the ECG lead (injected current (0.5-5m A safety current) to pick up this change. This change chart of respiratory impedance value describes the dynamic waveform of breathing, and can extract breathing parameters for monitoring the number of breaths per minute of the monitored person. Because the impedance value between the two breathing electrodes is extremely susceptible to the patient's severe and continuous body movement, speech, and outside contact interference, the measured value is often biased. In addition, the prone position on the side sometimes results in a small change in the resistance between the two breathing electrodes and no breathing value can be measured. It is also necessary to pay attention to the measurement, the chest impedance method is used for measurement, the measurement leads should be pulled apart as much as possible.

3) MEASUREMENT OF BLOOD PRESSURE

We know that the measured output of the blood pressure sensor is a mixed signal of pulse wave signal and cuff static pressure signal. After the pre-amplification, the pulse wave signal and the cuff static pressure signal are signals in two different frequency bands. The mixed signal after the pre-amplification needs to be divided into two channels. The low-pass filtering and band-pass filtering are performed separately to obtain the pulse wave oscillation signal and the cuff static pressure signal.

The output signal of the blood pressure sensor MPS3117-006GA is a differential signal, which is sent to a preamplifier circuit for amplification. Because the output differential signal is very weak, only a few tens of mV or less, the AD620 instrumentation amplifier is selected here to form a typical instrumentation amplifier circuit for primary amplification of the weak signal output by the sensor.

4) PULSE MEASUREMENT

Pulse is one of the most basic and important physiological parameters of the human body. At present, there are many methods for measuring pulse, so there are also many kinds of sensors for measuring weak pulse signals in the human body, such as Doppler effect sensors, photoelectric pair sensors and piezoelectric ceramic sensors. This system chooses a new polymer piezoelectric material PVDF (Polyvinylidene Fluoride) based piezoelectric sensor SC0073. SC0073 is a low-cost, high-performance miniature dynamic micro-pressure sensor with high sensitivity, simple structure, and weak pulse signals are accurately measured. The measuring principle of SC0073 dynamic micro-pressure sensor is: using PVDF piezoelectric film as a transducer, the dynamic micro-pressure signal is transmitted to the transducer through a special matching layer to become a charge, and then passes through the sensor. The amplifier circuit is converted into a voltage signal for transmission.

The pulse sensor uses a dynamic micro-pressure sensor SC0073 based on a PVDF piezoelectric film. SC0073 has 2 pins and can be used normally with an external load resistor and power supply, so the pulse signal acquisition circuit is relatively simple. In this system, the pulse signal collection site is the pulse beat of the human body.

After the weak pulse signal is collected by the sensor, it cannot be directly received by the back-end CC2430 main controller. The collected pulse signal needs to be processed. The processing process mainly includes amplification, filtering, shaping, comparison and so on. In this paper, the pulse signal conditioning circuit is mainly composed of several parts, such as an adaptive amplifier circuit, a notch circuit, a low-pass filter circuit, and a hysteresis comparison circuit.

Since any small change in the input voltage of the single-limit comparison circuit near the threshold voltage will cause a jump in the output voltage, the anti-interference ability is relatively poor. The voltage comparison circuit here uses a hysteresis comparison circuit. From the principle and performance of PVDF piezoelectric thin film materials, we know that SC0073 sensor based on PVDF piezoelectric thin film has good piezoelectric effect, and the thermoelectric effect is also obvious. In the past, the pulse sensors based on PVDF piezoelectric film on the market did not consider its temperature effect. The main reason was that the body temperature was basically constant. However, it was found in the experiment that although the body temperature of the human body basically changes within a small range, the temperature of the skin surface of the wrist pulse beat part is still affected by the external temperature change. The temperature difference of the skin of the site will also affect the measurement result to a certain extent. Therefore, the design of the filter circuit in the pulse signal conditioning circuit of this system fully considers the effect of the temperature effect. By using the frequency difference between the temperature signal (below 0.5Hz) and the human pulse (around 1Hz), it can basically be avoided.

5) MEASUREMENT OF BLOOD OXYGEN SATURATION

SpO_2 represents the concentration of O_2 in human blood and is an important parameter of the respiratory cycle. Currently, finger-type photoelectric sensors are widely used for the measurement of SpO_2. The blood oxygen saturation sensor is placed on the finger, and the finger is used as a transparent container for hemoglobin. The two light emitting diodes fixed on the upper arm emit infrared light as the incident light source. The photosensitive receiving device of the lower arm will pass the red light and the infrared light signal is converted into an electrical signal. According to the strength of the detected electrical signal, the value of the blood oxygen saturation can be calculated. We know that hemoglobin includes oxygenated hemoglobin HbO_2 (Oxygenated hemoglobin) and reduced hemoglobin Hb (Hemoglobin). Blood oxygen saturation refers to the percentage of the total hemoglobin content that can be combined with oxygen in the blood, namely:

$$SaO_2 = \frac{C_{HbO_2}}{C_{Hb} + C_{HbO_2}} \cdot 100\% \tag{3}$$

Among them, C_{HbO_2} represents the concentration of oxygenated hemoglobin, C_{Hb} represents the concentration of reduced hemoglobin, and the total hemoglobin concentration is added by the concentration of the two.

In this system, the blood oxygen saturation sensor uses the adult finger clip type non-invasive blood oxygen saturation probe DS100A developed by Nellcor. SpO_2 probe refers to the clip-on type. When using the SpO_2 probe on your finger, its interface adopts the serial port interface format, and the serial port of the supporting interface is used for connection. The oximeter probe interface has only 7 pins, and the definition of the pins is completely irrelevant to the serial port.

When the blood oxygen saturation needs to be measured, the LED light source constant current driving circuit drives the red light and the infrared light-diode in a time-sharing manner, so that they emit light at a lower duty

cycle and a certain time interval. According to the ratio of the light-emitting intensity of the infrared photodiode and the transmitted light received by the photodiode, the whole blood absorption rate of infrared light X905 can be calculated. With the help of the empirical formula of the quadratic function of blood oxygen saturation, the blood oxygen value can be calculated. The empirical formula for the quadratic function relationship of blood oxygen saturation is generally:

$$SaO_2 = A \cdot Q^2 + B \cdot Q + C \tag{4}$$

Among them, A, B, and C are constants and can be obtained by experimental calibration. Q represents the ratio of red light to infrared light. The empirical formula for the second-order function of blood oxygen saturation is obtained by the oximeter manufacturer in clinical experiments.

6) MEASUREMENT OF ECG SIGNALS

The ECG signal measurement method is to obtain the ECG signal on the surface of the human body through electrodes, and then send the obtained analog signal to the signal conditioning circuit, and then send it to the analog-to-digital converter after amplification and filtering to convert the analog signal into a digital signal. The microprocessor can further process the ECG signals converted into digital signals. Due to these characteristics of the ECG signal and the existence of various interference sources, in order to obtain high-quality ECG signals, the design requirements of the ECG signal conditioning circuit are very strict.

The main function of the ECG signal conditioning circuit is to amplify the weak ECG signal to a suitable size, which is convenient for the processing of the circuit, and then filter out the noise in the circuit with a filter circuit. The analog-to-digital converter converts the digital signal and sends the digital ECG signal to the microprocessor for further processing.

The BMD101 developed by Shennian Technology of the system uses a two-electrode single-lead input method. At the same time, an ESD electrostatic diode is added between the input electrode and the measurement chip to prevent electrostatic breakdown and burnout caused by excessive static electricity caused by the friction of clothing ECG acquisition chip. BMD101 has high requirements for power supply stability. Therefore, a π-shaped filtering method is used for the input end of the power supply. An independent power supply input VDD and a ground isolation circuit for limiting noise in the ECG signal are used to ensure the stability of the power supply.

At the same time, the digital ground and the analog ground of the system signal collection are electrically isolated to avoid introducing excessive power interference. The main and only communication interface of BMD101 is the serial interface of UART. The communication data format includes 1 stop, 1 start bit and 8 data bits. The ECG data can be transmitted to the MCU (Microcontroller Unit) directly through the serial port after being processed by the ECG algorithm inside the chip, eliminating the tedious process of the middle-class ECG acquisition system that relies too much on the MCU to process the pre-stage data and achieve a streamlined circuit. The design greatly simplifies the volume and redundancy of the hardware system. A filter capacitor and a decoupling capacitor are used between V_{CC} and GND to isolate digital and analog ground. So that the signal is not disturbed during transmission.

III. SIGNAL PROCESSING AND ALGORITHM DESIGN OF PHYSIOLOGICAL PARAMETERS

A. PROCESSING OF RESPIRATORY SIGNALS

1) DENOISING OF RESPIRATORY SIGNALS

By measuring the high-frequency voltage signal modulated by breathing, the change of human chest impedance is indirectly measured. At each measurement, a 100 kHz high-frequency signal is added to the human body, and then the impedance value of this measurement is calculated. Each time a high-frequency signal is loaded into the human body, due to the complexity of the human body and the uncertainty of external conditions, the high-frequency signal does not stabilize immediately. Therefore, the acquired chest impedance data is filtered based on median filtering to eliminate random noise and improve signal quality. The specific process is:

Each time the frequency scan is turned on, after the 100 kHz high-frequency signal is loaded on the human body, n values are continuously read for sorting from small to large, and then the intermediate value is taken as the result of this frequency scan. In order to make the breathing waveform smoother, the processed impedance data is subjected to sliding mean filtering.

2) CALCULATION OF RESPIRATORY RATE

Respiratory signals generally have the characteristics of rapid and smooth rise, large amplitude changes, and large differential values. As shown in Figure 3, a set of respiratory signals and their differential signals were measured by the impedance method. Because the rise of the respiratory waveform is not as obvious as the R wave of the ECG waveform, for the accuracy of peak detection, a dynamic differential threshold peak detection method is used to detect the peak of the respiratory waveform. After obtaining the peak-to-peak interval of the respiratory waveform, the respiratory rate can be calculated.

The specific process of dynamic differential threshold peak detection is as follows:

(1) Before processing the data, we select a certain length of data and divide the data into 5 segments, detect the maximum value of the difference and amplitude in each segment of data, remove the maximum and minimum values, and record the remaining difference and amplitude values respectively. For $C = [C_1, C_2, C_3]$ and $H = [H_1, H_2, H_3]$, C and H are averaged as C_0 and H_0, respectively. The initial differential threshold is set to $th_1 = 0.6C_0$, and the upper and lower limits of the amplitude threshold are set to $th_2 = 1.4H_0$ and $th_3 = 0.4H_0$, respectively.

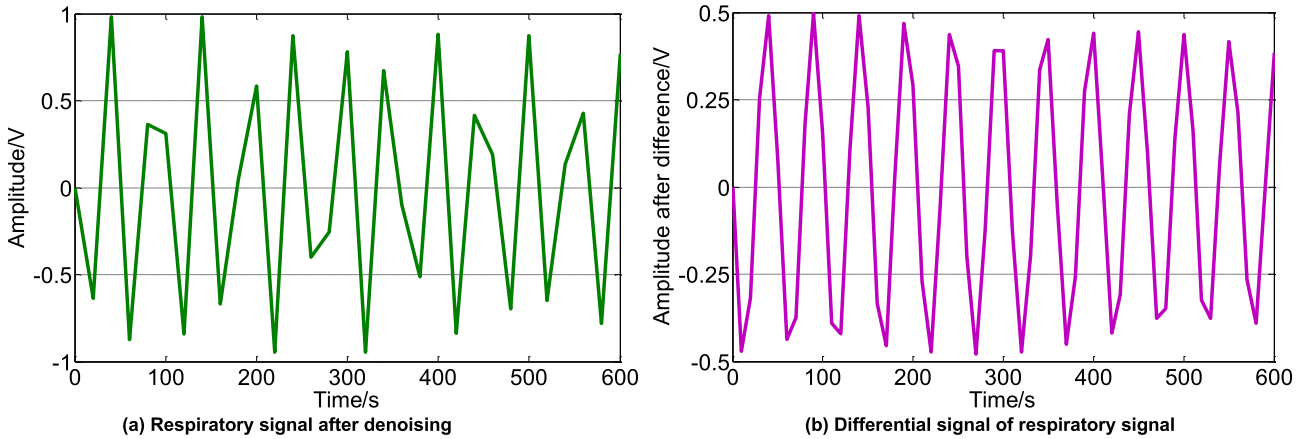

FIGURE 3. A respiratory signal and its differential signal.

(2) We use the initial threshold to start querying the peak point of the first breathing wave, and set the amplitudes of the points n_i, n_{i+1}, n_{i+2} to A_i, A_{i+1}, and A_{i+2} respectively. If it meets:

$$\begin{cases} th_1 < A_{i+1} - A_i \\ th_1 < A_{i+2} - A_{i+1} \end{cases} \tag{5}$$

Then the point n_{i+1} should be a point on the rising section of the breathing signal. Starting from the point n_{i+1}, the point of the differential zero crossing is found, which is a peak point corresponding to the breathing signal. If it meets:

$$\begin{cases} A_{k+3} \cdot A_{k+2} < 0 \\ A_{k+2} \cdot A_{k+1} > 0 \\ A_{k+1} \cdot A_k > 0 \end{cases} \tag{6}$$

Then n_{k+2} is a possible peak of the respiratory wave, and its amplitude is recorded as A_{new}. If A_{new} satisfies the following formula:

$$th_2 > A_{new} > th_3 \tag{7}$$

Then it is determined that n_{k+2} is a peak point; otherwise, the detection is continued.

(3) The threshold is updated after a new peak point is detected in the signal time series, and the next new peak point of the respiratory wave signal is detected according to the algorithm in process (2).

(4) We calculate the respiration rate based on the number of peak points detected within a certain period of time, and find the average of the peak-to-peak interval of the respiratory waveform over a period of time, and then calculate the respiration rate. The breathing rate calculation formula is as follows:

$$BR = \frac{60}{t'_{pp}} = \frac{60 \cdot f(n-1)}{N} \tag{8}$$

In the formula, t'_{pp} represents the average peak-to-peak interval, N represents the number of breath data separated by the position of the last breath wave peak and the position of the first breath wave, and n represents the number of breath wave peaks during this period, f is the sampling frequency of the respiratory data.

B. CUFFLESS ARTERIAL SYSTOLIC BLOOD PRESSURE FITTING ALGORITHM BASED ON PULSE WAVE TRANSIT TIME

PWTT (Pulse Wave Transit Time) refers to the time it takes for the pulse wave to travel from one point to another in the arteries. In this design, the time taken for the pulse wave to travel from the heart to the finger is used to represent PWTT. We select the feature points on the ECG waveform and the pulse wave waveform obtained by the finger, and calculate the time interval between the two feature points to find the time required for the pulse wave to reach the finger from the heart.

The velocity of the pulse wave in the blood vessel is affected by the thickness of the blood vessel and the elastic coefficient of the blood vessel wall. The relationship between them is:

$$v = \sqrt{\frac{gaE}{\rho d}} \tag{9}$$

In the formula, v is the pulse wave velocity, g is the acceleration of gravity; E is the elastic modulus of the blood vessel wall, ρ is the blood density, a is the thickness of the blood vessel wall, and d is the inner diameter of the blood vessel.

The relationship between the elastic modulus E and blood pressure is as follows:

$$v = E_0 e^{r \cdot SP} \tag{10}$$

In the formula, E_0 is the elastic modulus when the pressure is 0, γ is the vascular characteristic parameter, and SP is the systolic blood pressure. The relationship between pulse wave transit time and pulse wave velocity is as follows:

$$v = \frac{S}{PWTT} \tag{11}$$

In the formula, S is the pulse wave transmission distance.

The change in systolic blood pressure is inversely related to the change in pulse wave transit time, so there is the following relationship:

$$SP - SP_0 = \frac{2}{\gamma PWTT_0}(PWTT_0 - PWTT) \tag{12}$$

In the formula, SP_0 and SP are the systolic pressure in the initial state and the systolic pressure after the change; $PWTT_0$ and PWTT are the pulse wave pulse wave transmission time when the systolic pressure is SP_0 and the pulse wave pulse wave transmission time when the systolic pressure is SP.

The above formula can be simplified to:

$$SP = a \cdot PWTT + b \tag{13}$$

Among them, a and b are undetermined coefficients, and a and b are different between different individuals. For the same individual, a and b are almost unchanged within a certain range. The specific values of a and b can be determined by regression analysis.

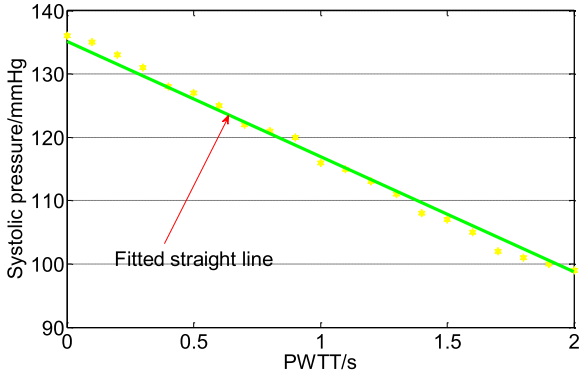

FIGURE 4. Relationship between pulse wave transit time and systolic blood pressure.

Figure 4 shows the relationship between the measured PWTT and systolic blood pressure of an individual. It can be seen that there is a strong correlation between PWTT and systolic blood pressure value, and the correlation coefficient is $R^2 = 0.94$.

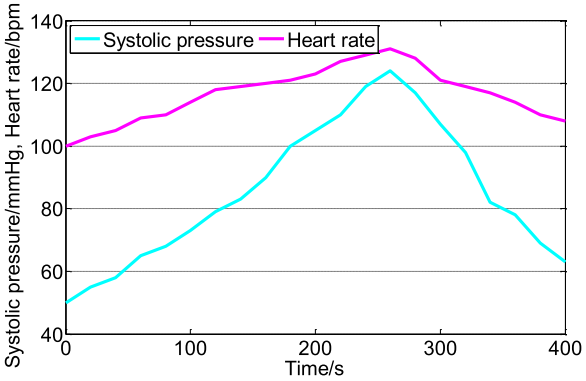

FIGURE 5. Continuous blood pressure measurement results.

Figure 5 shows the relationship between a continuously measured PWTT and systolic blood pressure. During the measurement, the subjects started squatting from the resting state, and remained at the resting state from t = 270s, and then we analyzed the obtained ECG and pulse wave data to obtain PWTT.

It can be seen from Figure 5 that the heart rate and blood pressure values have started to rise after starting the squat, and the heart rate and blood pressure values have started to decline after the squat movement has been stopped for 270s, which is consistent with human physiology. This proves the feasibility of PWTT-based calculation of human systolic blood pressure.

C. PULSE RATE AND BLOOD OXYGEN SATURATION VALUE CALCULATION

After the red light pulse wave signal and the infrared light pulse wave signal are preprocessed, most of the interference has been filtered out, and the blood oxygen saturation value and the pulse rate value can be obtained according to the calculation algorithm of the blood oxygen saturation. However, the pulse wave signal obtained by the reflection type oxygen saturation detection is weaker than the transmission type, and the stability is also worse. Therefore, it is necessary to design a stable calculation of the blood oxygen saturation and pulse frequency for the collected pulse wave signal. After analyzing the two pulse wave signals collected, it is found that the peak position is not stable, and small peaks are formed due to the blood flow rebound at the time when the aortic membrane is closed, which increases the difficulty of detecting the peaks. Because the crest is always between two valid troughs, the position of the crest can be determined by the position of the trough. At the same time, the intensity of the infrared light pulse wave signal is significantly stronger than that of the red light. Based on the above points, the algorithm flow chart for calculating the blood oxygen saturation and pulse rate is shown in Figure 6.

D. QRS WAVE DETECTION OF ECG SIGNALS

The electrocardiogram signal after wavelet transform denoising already has obvious QRS wave characteristic points, the waveform is clean, and the noise is small. It is an ideal signal for feature recognition. The QRS wave is the most obvious and useful signal among them, and it is also the basis for the electrocardiogram signal feature detection. The R wave signal has the largest forward amplitude and the steepest edge. Therefore, the position of the Q wave and S wave is generally obtained by detecting the position of the R wave peak. The pre-processed ECG signal has a good waveform and less noise. Therefore, after taking into account factors such as calculation volume and speed, the differential threshold method is used to extract QRS wave information.

1) R-WAVE AUTOMATIC DETECTION

The signal after differential processing reflects the slope information between two points of the original signal. The principle of the differential threshold method is to determine the position of the R wave according to the correspondence between the position of the signal singular point after the

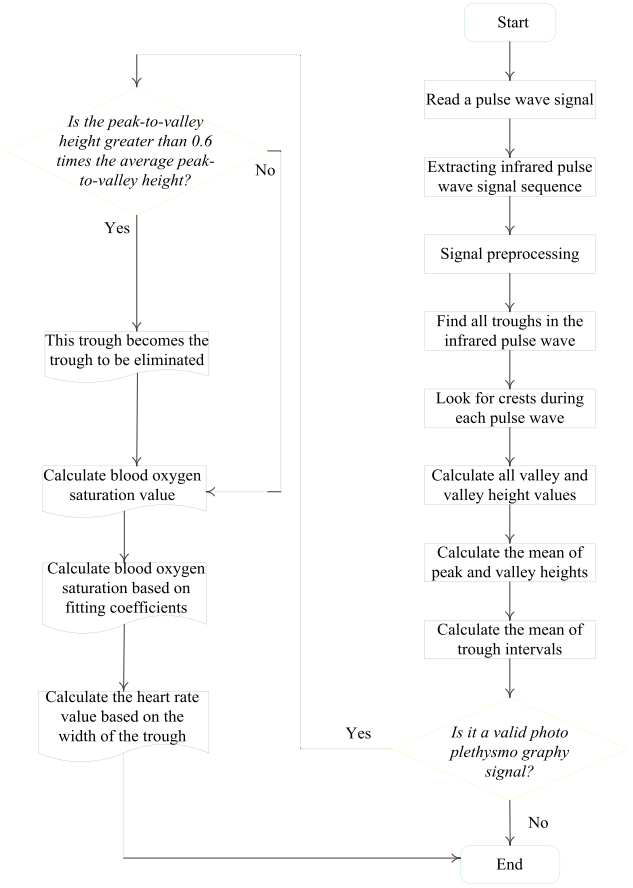

FIGURE 6. Pulse frequency and blood oxygen saturation calculation process.

ECG signal difference and the position of the original signal, which mainly includes two steps of difference operation and threshold judgment. The specific difference calculation methods are different. The difference calculation formula used here is:

$$dif(n) = 2f(n+2)+f(n+1)-f(n-1)-2f(n-2) \quad (14)$$

The result and the original signal after difference processing by the above formula are shown in Figure 7. On the whole, the difference signal amplifies the abrupt points of the original signal, making detection easier.

2) Q-WAVE AND S-WAVE DETECTION

Because the width of QRS waves in normal people is between 60ms and 100ms, and for patients with heart disease with bundle branch block or ventricular premature beats, the QRS wave width is generally greater than 100ms. Therefore, the R wave crest is used. A total of 140ms before and after the point is used as the detection range of Q wave and S wave. The detection process is as follows:

(1) Detection of Q wave valley points and S wave valley points: The first minimum value point found within 80ms forward is the Q wave valley point based on the position of the R wave peak point, which is the backward wave point; the first minimum point is the S wave trough point.

(2) Detecting the starting point of the Q wave and the ending point of the S wave: Finding the first zero-crossing point or the point closest to zero from the point of the Q wave trough is the starting point of the Q wave; the zero crossing or the point closest to zero is the end of the S wave.

IV. WIRELESS TELEMEDICINE SYSTEM TEST AND RESULT ANALYSIS

A. HUMAN BODY TEMPERATURE DETECTION TEST

The infrared temperature measurement module of the wireless remote medical system was used to measure the surface temperature of different parts of the human body, and compare with the contact thermocouple temperature measurement data. Here are 8 groups of repeated tests. The steps and requirements for each group are the same. The infrared temperature measurement module of the wireless remote medical system was used to measure the surface temperature of different parts of the human body, and compare with the contact thermocouple temperature measurement data. The comparison results of the 8 groups of tests are shown in Figure 8.

It can be seen from the measurement results that the error between the infrared temperature measurement result and the thermocouple temperature measurement result is small, which meets the temperature measurement requirements in the physiological parameter monitoring system.

In addition, in order to verify the stability of the temperature measurement system, a continuous temperature measurement test was performed. The continuous temperature measurement test was performed on the same person within 300s. Figure 9 shows the continuous temperature measurement results. It can be seen from the figure that the continuous temperature measurement results change within the range of 35 °C to 36 °C, which indicates that the temperature measurement system has a certain stability.

B. BREATHING SIGNAL DETECTION TEST

1) RESPIRATORY WAVEFORM RECORDING TEST

In order to verify the accuracy of the system's real-time monitoring of respiratory waveforms, an in-vivo breathing test was performed using the system. Six volunteers (numbered J1 ∼ J6) were selected for the test. The average age was 26 years old, including 4 men (J1 ∼ J4) and 2 women (J5 and J6). The volunteers were healthy, fully informed and consented to the trial. During the test, the chest strap was placed on the volunteer's chest. The volunteer held their breath for the first 5 s and then breathed normally. The entire test lasted 20 s. Figure 10 shows the results of real-time respiration measurements on six volunteers.

As can be seen from Figure 10 the measurement results accurately reflected the waveforms of the breath holding state and normal breathing state of the 6 volunteers during the test.

2) RESPIRATION RATE TEST

The peak detection technology of dynamic differential threshold method is used to extract the peak point from the breathing

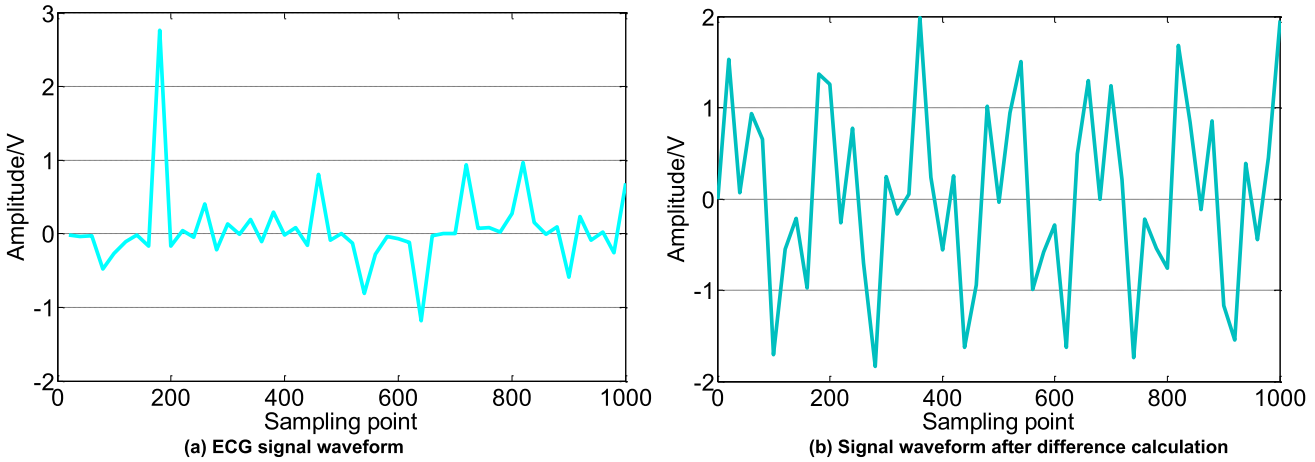

FIGURE 7. Comparison of ECG signal waveform and signal waveform after differential operation.

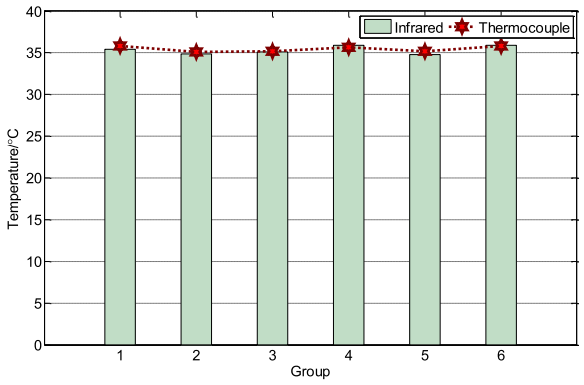

FIGURE 8. Human skin temperature measurement results.

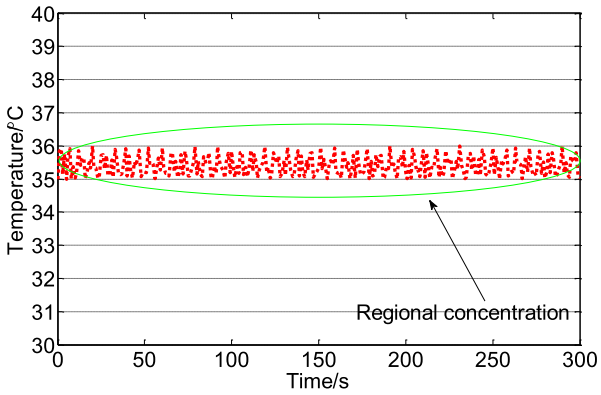

FIGURE 9. Results of continuous temperature measurement test.

waveform, and the value of the breathing rate is obtained. In order to verify the dynamic difference threshold peak detection algorithm, this experiment is designed. Six volunteers (numbered L1 to L6) were selected in the experiment, with an average age of 26 years, including three males (L1 to L3) and three females (L4 to L6). The volunteers were healthy, fully informed and consented to the trial. In the test, each volunteer was given five normal breaths, the breath times were 10, 50, 100, 200, and 300. The respiratory data (numbered G1 to G5) were recorded, and the peak detection algorithm was used to record the records. 5 sets of respiratory data were processed. Figure 11 shows the detection results of the peak points of the respiratory signals of 5 groups of 6 volunteers.

It can be seen from Figure 11 that the accuracy rate of detecting peak points of 10 groups of respiratory signals is more than 97%, which indicates that the detection results are more accurate. Therefore, the respiration rate can be accurately calculated based on the peak detection result, which meets the requirement of real-time detection of the respiration rate by physiological parameter detection equipment.

C. BLOOD PRESSURE MEASUREMENT TEST

In order to verify the cuff-free blood pressure measurement algorithm, this test was designed. The test equipments are the human multiple physiological parameter monitoring system and Mindray's iMEC10 multiple physiological parameter monitor. The multi-physiological parameter monitoring system measures the ECG and pulse wave of the human body, and calculates the systolic and diastolic blood pressure of the human body by calculating the PWTT. The cuff-type sphygmomanometer that comes with the iMEC10 monitor is used to measure human blood pressure, and the measured blood pressure is used as the standard blood pressure control value.

Five volunteers (numbered L1 to L5) were selected in the experiment, with an average age of 25 years, including three men (L1 to L3) and two women (L4 and L5). The volunteers were healthy, fully informed and consented to the test. Before the test, the volunteers were kept at rest for 5 minutes. During the test, the volunteers' ECG and pulse wave waveforms were collected first, and then the blood pressure was measured with the blood pressure meter provided by Mindray iMEC10 monitor. The average of the remaining three measurements is

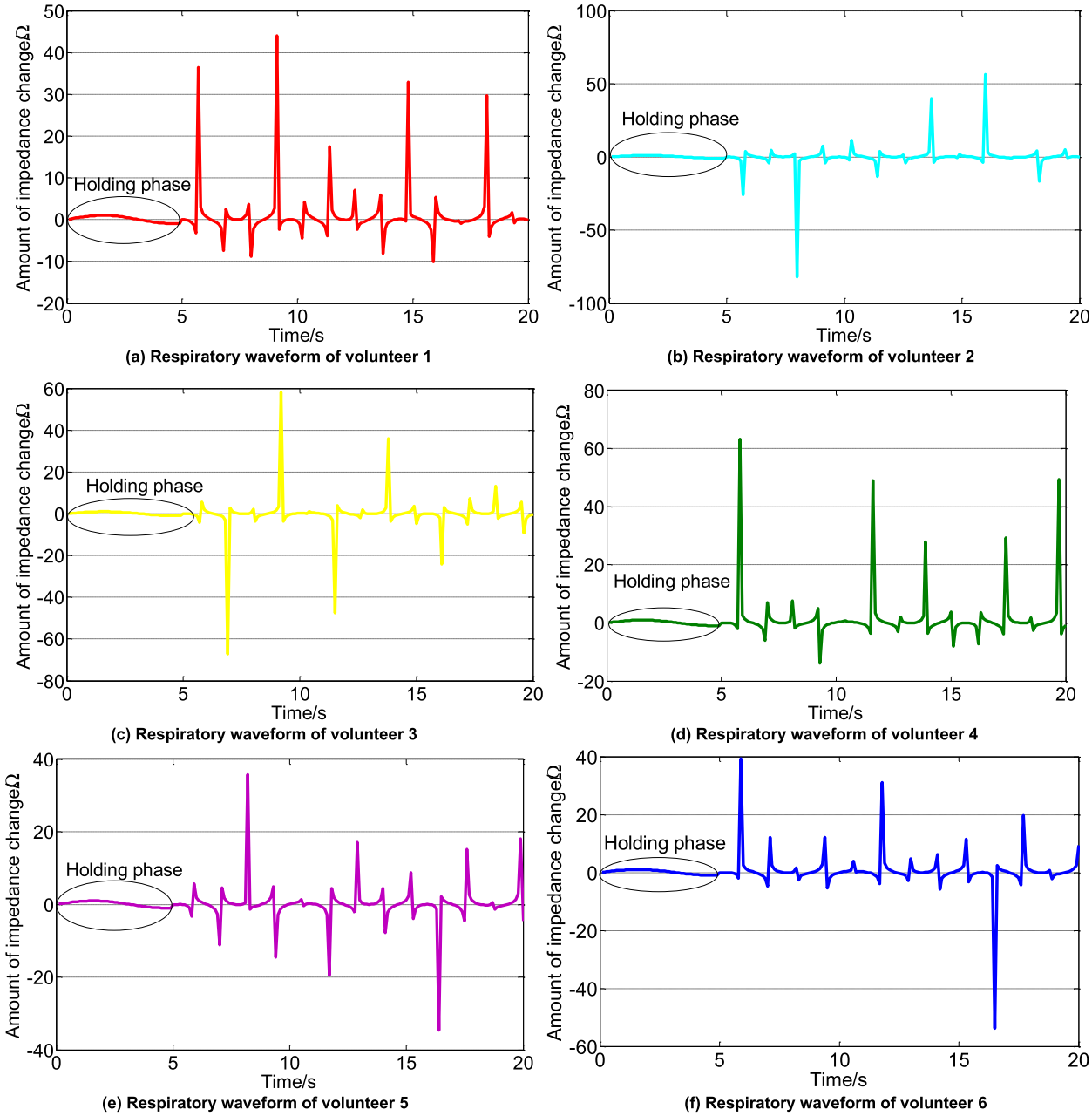

FIGURE 10. Results of real-time breath measurement test of 6 volunteers.

taken as the measurement result of this test. We repeat the test procedure five times at five minute intervals and record the test results. The measurement results of five volunteers are shown in Table 1. It can be seen from Table 1 that the measurement results of the two blood pressure detection methods are consistent. Therefore, the blood pressure measurement method without a cuff based on the pulse wave transit time meets the blood pressure measurement requirements of the human multiple physiological parameter monitoring system.

D. PULSE OXIMETRY TEST

In order to verify the accuracy of pulse signal monitoring, this test was designed. The reflective pulse oximetry module was fixed at the end of the index finger of the human body, and the collected signal was processed and sent to the upper position for processing. The pulse wave waveform and blood oxygen were displayed. The volunteers in the test are members of the project team. He is 26 years old and in good health, and is fully informed and consents to the test. Volunteer was in a quiet state during the test, and the reflective pulse oximetry module and the photoelectric finger clip of the Mindray monitor were fixed to the index finger and middle finger of the left hand.

As shown in Figure 12, waveform 1 is the pulse wave waveform measured by the reflective pulse oximetry module of the system, and waveform 2 is the pulse wave waveform

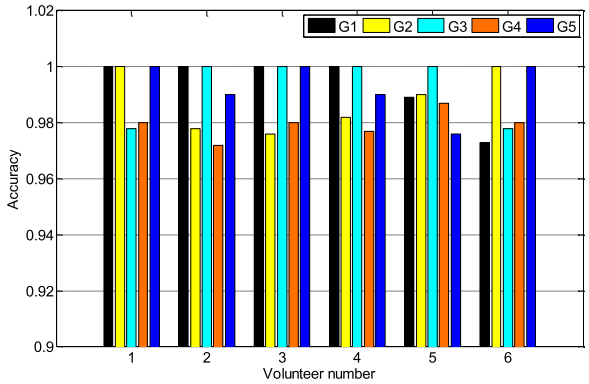

FIGURE 11. Peak point detection results.

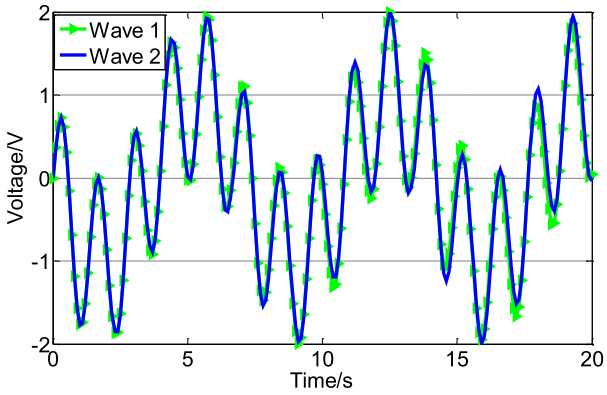

FIGURE 12. Pulse wave waveform.

TABLE 1. Blood pressure measurement test results.

Numbering	iMEC10 measured value		Values measured by this system	
	Systolic pressure	Diastolic pressure	Systolic pressure	Diastolic pressure
L1	109	73	109	73
L2	114	71	113	70
L3	108	69	108	69
L4	110	76	110	75
L5	117	74	116	74

measured by Mindray Life Monitor. It can be seen that waveform 1 and waveform 2 are basically the same.

In order to verify the accuracy and applicability of the blood oxygen saturation detection algorithm, this experiment was designed. Five volunteers (numbered L1 to L5) were selected in the test, with an average age of 25 years, including four males (L1 to L4) and one female (L5). In the test, each volunteer measured the blood oxygen saturation of the human body in a quiet state and in a radon state. Table 2 shows the measurement results.

In the table, A represents the blood oxygen saturation measured by the multiple physiological parameter detection system, and B represents the blood oxygen saturation measured by Mindray iMEC10 in the same state. It can be seen from

TABLE 2. Accuracy of blood oxygen saturation measurement test (%).

Numbering	Normal status		Radon 30s		Radon 50s	
	A	B	A	B	A	B
L1	98	98	97	97	96	97
L2	97	97	98	98	95	95
L3	98	98	96	96	95	95
L4	99	99	98	99	97	97
L5	99	98	97	97	94	94

Table 2 that the blood oxygen saturation results measured by the human multi-physiological parameter monitoring system are basically the same as those of Mindray iMEC, and under the belching state, it can accurately reflect the downward trend of bleeding oxygen saturation.

E. ECG SIGNAL MEASUREMENT TEST

1) ECG WAVEFORM MEASUREMENT TEST

In order to verify whether the ECG acquisition module can accurately measure the ECG waveform, this experiment was designed. One volunteer, 24 years old, was selected for the test. The volunteers were in good health and fully informed and agreed to the test. Figure 13 shows a set of measured electrocardiogram waveforms. It can be seen from the figure that the waveform quality of this group of electrocardiogram is good, high frequency noise and baseline drift are filtered out, and the ECG signal acquisition module works normally, meeting the requirements of ECG signal acquisition.

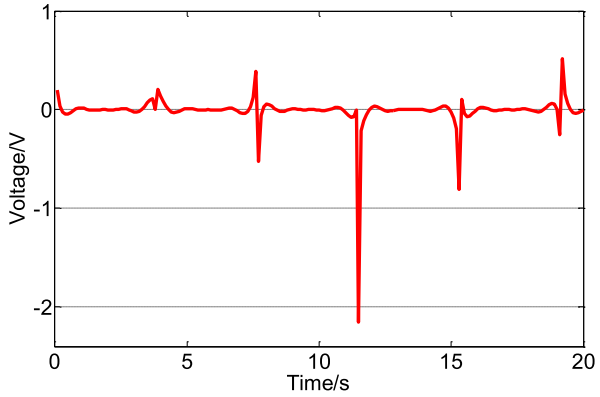

FIGURE 13. Measured ECG waveform.

2) HEART RATE TEST

Heart rate calculation is calculated by the number of R waves over a period of time. Therefore, the accuracy of the R-wave detection determines the accuracy of the heart rate calculation. In order to verify the R-wave detection algorithm, this experiment was designed. Five volunteers (numbered L1 to L5) were selected in the test, with an average age of 24 years, including three males (L1 to L3) and two females (L4 and L5). The volunteers were healthy, fully informed

and consented to the test. During the test, the ECG data of the volunteers were measured for 2 minutes in the quiet state and 5 minutes after the light exercise, and the R-wave detection test was performed on the measured data using the R-wave detection method. Table 3 shows the detection results of 5 groups of peaks of 5 volunteers.

TABLE 3. R wave peak point detection results.

Numbering	R-wave detection accuracy after light exercise (%)	R-wave detection accuracy in quiet state (%)
L1	97.2	98.4
L2	98.5	99.6
L3	99.3	99.8
L4	99.8	98.3
L5	97.6	98.7

It can be seen from Table 3 that the accuracy of the R wave detection of the ECG signal is more than 97%, and the detection result is accurate. The heart rate can be accurately calculated based on the peak detection results, which meets the requirements of real-time heart rate detection by physiological monitoring equipment. In further research, the online user database of medical institutions can be accessed through the mobile Internet to achieve electronic medical record synchronization, online reporting and diagnosis.

V. CONCLUSION

Based on the research of wireless communication technology and telemedicine application status, this paper expounds the feasibility and promotion value of the development of telemedicine monitoring technology, and proposes a multi-physical parameter wireless telemedicine health monitoring system solution. The system mainly measures six physiological parameters of human medical monitoring, namely body temperature, respiration, blood oxygen saturation, pulse, blood pressure and ECG. The digital filtering algorithm of human physiological signals is completed, which improves the quality of the collected physiological signals. The detection algorithms of heart rate, respiration rate, and blood oxygen saturation were completed, and the accurate detection of heart rate, respiration rate, and blood oxygen saturation was achieved. In order to reduce the influence of blood oxygen saturation on the daily activities of people, a reflective design is adopted. In view of the large individual variation and unstable characteristics of photoelectric volume pulse wave signals obtained by reflective blood oxygen detection, a more applicable blood oxygen saturation calculation algorithm is designed in this paper, and its threshold is obtained through adaptive learning. In order to accurately extract the QRS feature points of the ECG signal, a differential threshold method is used and false detection and missed detection mechanisms are added. Using Mindray's iMEC10 patient multi-physiological parameter monitor and multi-physiological parameter health monitoring system for comparison test, the error analysis and discussion of the test data verify the accuracy and reliability of the system. However, when analyzing and storing the physiological parameters of the human body, the speed of analysis by the monitoring terminal is not fast enough. Once the amount of data is too large, it will inevitably cause the data to be transmitted in a timely manner. How to accelerate the speed of data analysis remains to be studied.

REFERENCES

[1] M. Manas, A. Sinha, S. Sharma, and M. R. Mahboob, "A novel approach for IoT based wearable health monitoring and messaging system," *J. Ambient Intell. Humanized Comput.*, vol. 10, no. 7, pp. 2817–2828, Jul. 2019.
[2] R. Punj and R. Kumar, "Technological aspects of WBANs for health monitoring: A comprehensive review," *Wireless Netw.*, vol. 25, no. 3, pp. 1125–1157, 2019.
[3] A. Manirabona and L. C. Fourati, "A 4-tiers architecture for mobile WBAN based health remote monitoring system," *Wireless Netw.*, vol. 24, no. 6, pp. 2179–2190, Aug. 2018.
[4] I. Nishidate, M. Minakawa, D. McDuff, M. A. Wares, K. Nakano, H. Haneishi, Y. Aizu, and K. Niizeki, "Simple and affordable imaging of multiple physiological parameters with RGB camera-based diffuse reflectance spectroscopy," *Biomed. Opt. Express*, vol. 11, no. 2, pp. 1073–1091, Feb. 2020.
[5] R. Shanthapriya and V. Vaithianathan, "Secured healthcare monitoring system in wireless body area network using polynomial based technique," *Polish J. Med. Phys. Eng.*, vol. 25, no. 3, pp. 171–177, Sep. 2019.
[6] B. Raja, A. Firdous, A. M. Ishak, and M. Anand, "Design and implementation of health care video monitoring system based on RTOS," *Indian J. Public Health Res. Develop.*, vol. 10, no. 4, pp. 1260–1265, 2019.
[7] A. Misra, P. Agnihotri, and J. K. Dwivedi, "Advanced IoT based combined remote health monitoring and alarm system," *Int. J. Advance Res. Develop.*, vol. 3, no. 4, pp. 6–11, 2018.
[8] A. H. Abdulwahid, "Modern application of Internet of Things in healthcare system," *Int. J. Eng. Res. Technol.*, vol. 12, no. 4, pp. 494–499, 2019.
[9] S. Senthilkumar, K. Brindha, R. Charanya, and A. Kumar, "Patients health monitoring system using IOT," *Indian J. Public Health Res. Develop.*, vol. 10, no. 4, pp. 252–256, 2019.
[10] S.-S. Lin and J.-J. Lin, "Development of a novel health promotion system based on wireless sensor network and cloud computing," *Sensors Mater.*, vol. 31, no. 3, pp. 939–952, Mar. 2019.
[11] L. P. Malasinghe, N. Ramzan, and K. Dahal, "Remote patient monitoring: A comprehensive study," *J. Ambient Intell. Humanized Comput.*, vol. 10, no. 1, pp. 57–76, Jan. 2019.
[12] Y. Li, L. Zheng, and X. Wang, "Flexible and wearable healthcare sensors for visual reality health-monitoring," *Virtual Reality Intell. Hardw.*, vol. 1, no. 4, pp. 411–427, Aug. 2019.
[13] A. Prati, C. Shan, and K. I.-K. Wang, "Sensors, vision and networks: From video surveillance to activity recognition and health monitoring," *J. Ambient Intell. Smart Environ.*, vol. 11, no. 1, pp. 5–22, 2019.
[14] S. Raja, "Chronic health patient monitoring system using IOT," *Int. J. Recent Innov. Trends Comput. Commun.*, vol. 6, no. 3, pp. 114–119, 2018.
[15] M. Al-khafajiy, T. Baker, C. Chalmers, M. Asim, H. Kolivand, M. Fahim, and A. Waraich, "Remote health monitoring of elderly through wearable sensors," *Multimedia Tools Appl.*, vol. 78, no. 17, pp. 24681–24706, Sep. 2019.
[16] A. Bashir and A. H. Mir, "Secure framework for Internet of Things based e-health system," *Int. J. E-Health Med. Commun.*, vol. 10, no. 4, pp. 16–29, Oct. 2019.
[17] P. Verma and S. K. Sood, "A comprehensive framework for student stress monitoring in fog-cloud IoT environment: M-health perspective," *Med. Biol. Eng. Comput.*, vol. 57, no. 1, pp. 231–244, Jan. 2019.
[18] J. Kim, A. S. Campbell, B. E.-F. de Ávila, and J. Wang, "Wearable biosensors for healthcare monitoring," *Nature Biotechnol.*, vol. 37, no. 4, pp. 389–406, Apr. 2019.
[19] B. Xu, L. Xu, H. Cai, L. Jiang, Y. Luo, and Y. Gu, "The design of an m-Health monitoring system based on a cloud computing platform," *Enterprise Inf. Syst.*, vol. 11, no. 1, pp. 17–36, 2017.

[20] H. Rahman, M. U. Ahmed, and S. Begum, "Non-contact physiological parameters extraction using facial video considering illumination, motion, movement and vibration," *IEEE Trans. Biomed. Eng.*, vol. 67, no. 1, pp. 88–98, Jan. 2020.
[21] K. Suriyakrishnaan and D. Sridharan, "Reliable packet delivery in wireless body area networks using TCDMA algorithm for e-health monitoring system," *Wireless Pers. Commun.*, vol. 103, no. 4, pp. 3127–3144, Dec. 2018.
[22] G. Lazzi, R. Lee, and K. S. Nikita, "Guest editorial for the special issue on wireless real-time health monitoring technology for personalized medicine," *IEEE Trans. Antennas Propag.*, vol. 67, no. 8, pp. 4946–4954, Aug. 2019.
[23] A. Ahmed, A. A. Lukman, A. James, O. O. Mikail, B. U. Umar, and E. Samuel, "Human vital physiological parameters monitoring: A wireless body area technology based Internet of Things," *J. Teknologi Dan Sistem Komputer*, vol. 6, no. 3, pp. 115–121, Jul. 2018.
[24] B. Sharma and D. Koundal, "Cattle health monitoring system using wireless sensor network: A survey from innovation perspective," *IET Wireless Sensor Syst.*, vol. 8, no. 4, pp. 143–151, Aug. 2018.
[25] S. Vaishnodevi, S. Mathankumar, G. Ramachandran, and A. Malarvizhi, "Wireless based human health monitoring and fall detection using GSM," *Indian J. Public Health Res. Develop.*, vol. 9, no. 11, pp. 1541–1544, 2018.
[26] G. H. Khan, A. P. Manwatkar, and N. P. Khan, "Real-time IOT-based health care monitoring for prediction and analysis," *Our Heritage*, vol. 68, no. 30, pp. 217–220, 2020.
[27] G. V. Vinod, V. Lavanya, V. Ramana, and D. Bhavani, "Automatic monitoring of human body physiological parameters using lab VIEW," *Indian J. Public Health Res. Develop.*, vol. 9, no. 12, pp. 1570–1574, 2018.
[28] A. H. Sodhro, A. S. Malokani, G. H. Sodhro, M. Muzammal, and L. Zongwei, "An adaptive QoS computation for medical data processing in intelligent healthcare applications," *Neural Comput. Appl.*, vol. 32, no. 3, pp. 723–734, Feb. 2020.
[29] S. Gahlot, S. R. N. Reddy, and D. Kumar, "Review of smart health monitoring approaches with survey analysis and proposed framework," *IEEE Internet Things J.*, vol. 6, no. 2, pp. 2116–2127, Apr. 2019.
[30] I. Masood, Y. Wang, A. Daud, N. R. Aljohani, and H. Dawood, "Privacy management of patient physiological parameters," *Telematics Informat.*, vol. 35, no. 4, pp. 677–701, Jul. 2018.
[31] E. Jafer, S. Hussain, and X. Fernando, "A wireless body area network for remote observation of physiological signals," *IEEE Consum. Electron. Mag.*, vol. 9, no. 2, pp. 103–106, Mar. 2020.
[32] G. P. Samuel, C. D. Naidu, and S. Chettineni, "A probably secure WiFi based health monitoring system through assymetric cryptography (RSA) using embedded applications," *Int. J. Appl. Eng. Res.*, vol. 13, no. 11, pp. 9288–9293, 2018.
[33] C. U. Devi, T. V. Prasad, K. Jyotsna, and M. Madhavi, "IoT based health care monitoring system using wireless sensor networks," *Indian J. Public Health Res. Develop.*, vol. 9, no. 12, pp. 1579–1583, 2018.
[34] C. Shao, Q. Zhang, Y. Song, and D. Zhu, "Smart home healthcare system based on middleware and counter neural network," *J. Med. Imag. Health Inform.*, vol. 10, no. 5, pp. 1105–1112, May 2020.
[35] S. Suryanarayanan, S. Manmadhan, and N. Rakesh, "Design and development of real time patient monitoring system with GSM technology," *J. Cases Inf. Technol.*, vol. 19, no. 4, pp. 22–36, Oct. 2017.
[36] Y. Li, P. Liu, Q. Cai, J. Guo, Z. Zhou, H. Yan, M. Qian, F. Yu, K. Yuan, and J. Yu, "A health gateway for mobile monitoring in nursing home," *Wireless Pers. Commun.*, vol. 102, no. 2, pp. 1573–1587, Sep. 2018.
[37] A. Alameen and A. Gupta, "Optimization driven deep learning approach for health monitoring and risk assessment in wireless body sensor networks," *Int. J. Bus. Data Commun. Netw.*, vol. 16, no. 1, pp. 70–93, Jan. 2020.
[38] P. Verma, S. K. Sood, and S. Kalra, "Cloud-centric IoT based student healthcare monitoring framework," *J. Ambient Intell. Humanized Comput.*, vol. 9, no. 5, pp. 1293–1309, Oct. 2018.
[39] M. V. Suganthi, M. K. Elavarasi, and M. J. Jayachitra, "Tele-health monitoring system in a rural community through primary health center using Internet of medical things," *Int. J. Pure Appl. Math.*, vol. 119, no. 14, pp. 695–703, 2018.
[40] N. Bavya, T. Arunkumar, and K. Adalarasu, "A comprehensive survey on IoT technologies in health care system," *Res. J. Pharmacy Technol.*, vol. 11, no. 7, pp. 3157–3162, 2018.
[41] N. Yessad, M. Omar, A. Tari, and A. Bouabdallah, "QoS-based routing in wireless body area networks: A survey and taxonomy," *Computing*, vol. 100, no. 3, pp. 245–275, Mar. 2018.
[42] L. Yang, Y. J. Zhou, C. Zhang, X. M. Yang, X.-X. Yang, and C. Tan, "Compact multiband wireless energy harvesting based battery-free body area networks sensor for mobile healthcare," *IEEE J. Electromagn., RF Microw. Med. Biol.*, vol. 2, no. 2, pp. 109–115, Jun. 2018.
[43] X. Zhao, V. Sadhu, T. Le, D. Pompili, and M. Javanmard, "Toward wireless health monitoring via an analog signal compression-based biosensing platform," *IEEE Trans. Biomed. Circuits Syst.*, vol. 12, no. 3, pp. 461–470, Jun. 2018.
[44] K. Gürkan, G. Gürkan, and A. A. Dindar, "Design and realization of multichannel wireless data acquisition system for laboratory-scale experiments on structural health monitoring," *J. Meas. Eng.*, vol. 6, no. 1, pp. 64–73, Mar. 2018.
[45] S. M. Thaung, H. M. Tun, K. K. K. Win, M. M. Than, A. S. S. Phyo, A. Mon, S. H. Pha, C. Tin, S. A. Y. Oo, and T. T. Hla, "Exploratory data analysis based on remote health care monitoring system by using IoT," *Communications*, vol. 8, no. 1, pp. 1–8, 2020.

KAI ZHANG was born in Henan, China, in 1980. He received the bachelor's and master's degrees from Henan Normal University, in 2003 and 2010, respectively. He currently works with Xinxiang Medical University. His research directions are sports and health.

WENJIE LING was born in Henan, China, in 1973. He received the master's degree in education from Henan University, in 2001. He is currently an Associate Professor with Xinxiang Medical University. He has published more than 60 articles, supported two provincial projects, three departmental projects, and edited three textbooks. His research interests include sports and health, rural sports, and school sports.